# Threshold PCA denoising outperforms MP-PCA in Correlation Tensor Imaging data of human brain microstructure at 3T

Manu Raghavan[a], Lisa Novello[b], Rafael Neto Henriques[c], Noam Shemesh[c], Andrada Ianuş[d], Thorsten Feiweier[e], Domenico Zacà[f], Jorge Jovicich[a]

[a]*Centre for Mind/Brain Sciences - CIMeC, University of Trento, Rovereto, Italy*

[b]*Data Science for Health (DSH) Research Unit, Fondazione Bruno Kessler, Trento, Italy*

[c]*Champalimaud Research, Champalimaud Foundation, Lisbon, Portugal*

[d]*Biomedical Engineering and Imaging Sciences, King's College London, London, United Kingdom*

[e]*Research & Clinical Translation, Magnetic Resonance, Siemens Healthineers AG, Erlangen, Germany*

[f]*Siemens Healthcare, Milan, Italy*

## Introduction

Correlation Tensor Imaging (CTI) is an advanced diffusion MRI method based on Double-Diffusion-Encoding (DDE) that separates diffusional kurtosis into isotropic (Kiso), anisotropic (Kaniso), and microscopic (μK) components, offering greater specificity for brain microstructure characterization [1]. While CTI has shown strong potential in preclinical studies [2], and was recently demonstrated in humans [3], current protocols require long acquisitions (~50 min), limiting clinical feasibility. Accelerating CTI will drastically reduce acquisition time but also exacerbate signal-to-noise ratio (SNR) losses, making effective denoising crucial. PCA-based methods such as Marčenko-Pastur PCA (MP-PCA) [4] and Threshold PCA (TPCA) [5] have shown promise for denoising diffusion MRI data without compromising microstructural information. While MP-PCA denoising classifies principal components based on the Marčenko-Pastur distribution, assuming spatially uncorrelated noise, TPCA incorporates a prior estimate of the noise variance to establish a threshold for noise component removal, enhancing robustness in scenarios with spatially correlated noise. This study evaluates, for the first time, the effects of MP-PCA and TPCA denoising on CTI-derived metrics in healthy human brains.

**Methods:**

Population & MRI Acquisition: We used CTI data acquired from 8 healthy young volunteers, as described in a previous 3T study [3].

Preprocessing and CTI: Three CTI preprocessing pipelines (P1–P3) were implemented, differing only in their PCA denoising approach: P1 – no denoising; P2 – MP-PCA (MRtrix3) [4]; P3 – TPCA (Dipy) [5]. After denoising, all pipelines included the same subsequent corrections in the following order: Gibbs ringing (MRtrix3), geometric distortions and eddy currents (FSL), signal drift [6], and bias field (MRtrix3). CTI metrics were fitted and estimated within different brain regions of interest (ROIs).

Statistical Analysis: To assess the impact of denoising across different processing pipelines, we compared three key metrics within ROIs: 1) the mean CTI estimates, 2) the within-ROI variability of CTI values, and 3) the percentage of voxels with biologically implausible (i.e., negative) CTI fits. Statistical analysis was conducted using within-subject repeated measures. A Friedman test was first applied to identify overall effects of the pipeline. When significant, this was followed by right-tailed Wilcoxon signed-rank tests for pairwise pipeline comparisons. P-values were adjusted for multiple comparisons using the False Discovery Rate (FDR) method.

**Results**

**Figure 1** shows sample subject results from the three pipelines on CTI metrics. Denoising improvements are most visible on μK. At the group level, there were no significant differences across pipelines on CTI metrics averaged in the ROIs. When looking at within-ROI variability and percentage of negative CTI fits, we observed significant improvements with denoising, in particular with TPCA (**Table 1**). **Figure 2** shows how voxel-wise variability of CTI metrics is systematically and significantly reduced within the various ROIs considered when moving from P1 to P2 to P3, especially for μK ($p < 0.01$). In addition, we found similar effects of denoising improvements when looking at the percent of negative CTI model fits (biologically impossible values) within the various ROIs, especially for μK (**Figure 3**).

## Figures

### Fig 1

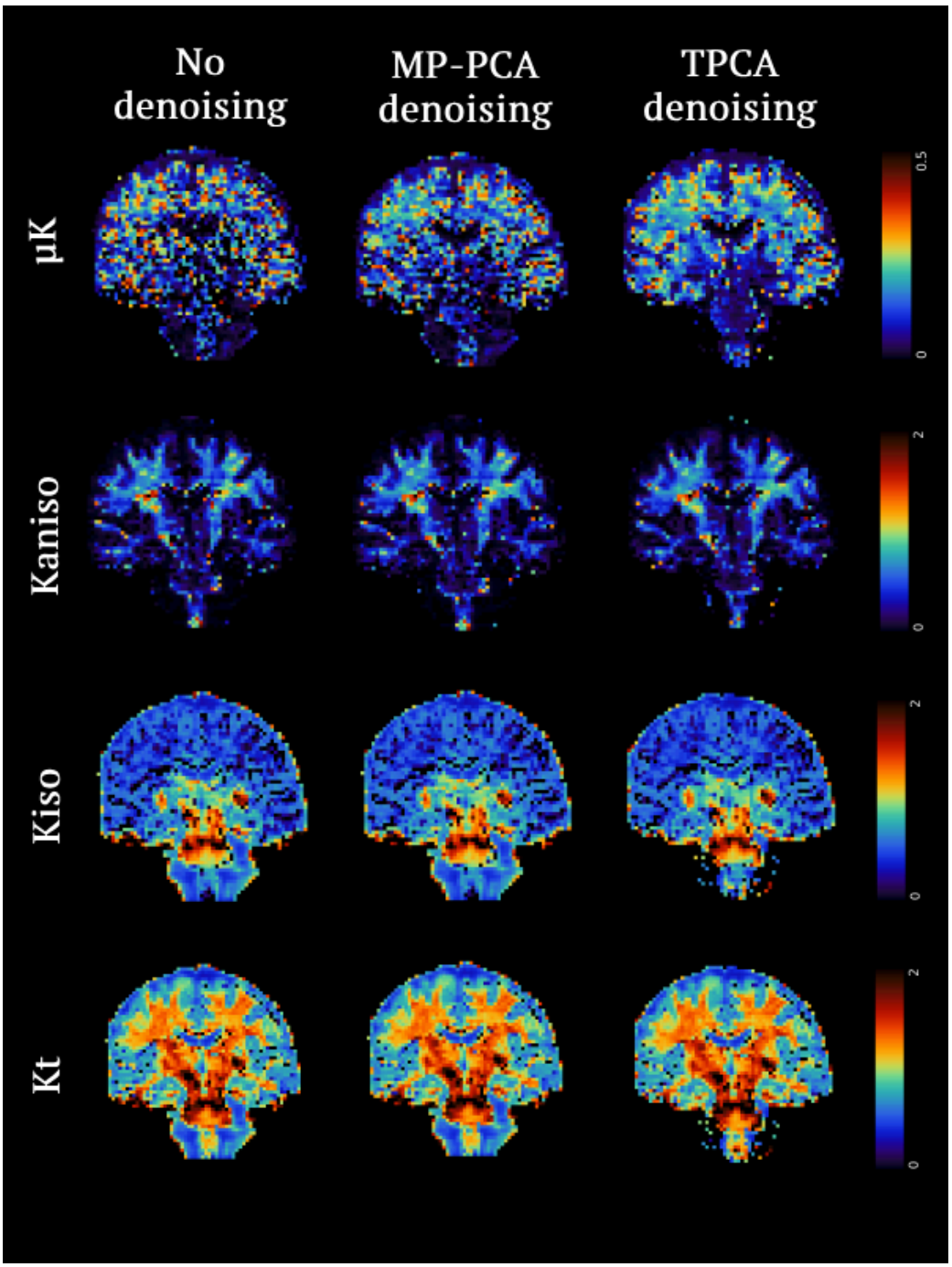


**Figure 1**. Single subject CTI derived maps of microkurtosis (μK), anisotropic kurtosis ($K_{aniso}$), isotropic kurtosis ( $K_{iso}$), and total kurtosis ($K_t$) across denoising pipelines.

### Table 1

a) Within-subject pipeline effects on voxel-wise variability

| CTI metrics | Friedman's test for pipeline effects (p<0.05) | Right-Tailed Wilcoxon Signed-Rank Test | | |
|---|---|---|---|---|
| | | P1>P2 | P1>P3 | P2>P3 |
| **Ktotal** | CSF | NS | NS | NS |
| **Kiso** | WM, CSF, GM, PU, HPC | PU, HPC (p<0.02) | WM, GM, PU (p<0.007) | WM, GM (p<0.02) |
| **Kaniso** | WM, GM, PU, HPC | WM, PU (p<0.01) | WM, GM, PU, HPC (p<0.02) | WM, GM, PU, HPC (p<0.05) |
| **μK** | CSF, WM, GM, PU, HPC | CSF, WM, GM, PU,HPC (p<0.004) | CSF, WM, GM, PU,HPC (p<0.004) | CSF, WM, GM, PU,HPC (p<0.008) |

b) Pipeline effects on percentage negative CTI fits

| CTI metrics | Friedman's test for pipeline effects (p<0.05) | Right-Tailed Wilcoxon Signed-Rank Test | | |
|---|---|---|---|---|
| | | P1>P2 | P1>P3 | P2>P3 |
| **Ktotal** | GM | GM (p<0.02) | NS | NS |
| **Kiso** | WM, GM | WM (p<0.05) | GM (p<0.05) | GM (p<0.05) |
| **Kaniso** | GM | NS | GM (p<0.05) | GM (p<0.01) |
| **μK** | CSF, WM, GM, PU, HPC | CSF, WM, GM, PU,HPC (p<0.008) | CSF, WM, GM, PU,HPC (p<0.004) | CSF, WM, GM, PU,HPC (p<0.004) |

**Table 1**. Statistical effects of denoising on voxel-wise variability (a) and % negative CTI fits (b). Abbreviations: CSF - Cerebrospinal Fluid, WM - White Matter, GM - Gray Matter, HPC - Hippocampus, PU - Putamen, NS - not significant. P1: No denoising, P2: MP-PCA denoising, P3: TPCA denoising.

**Fig 2**

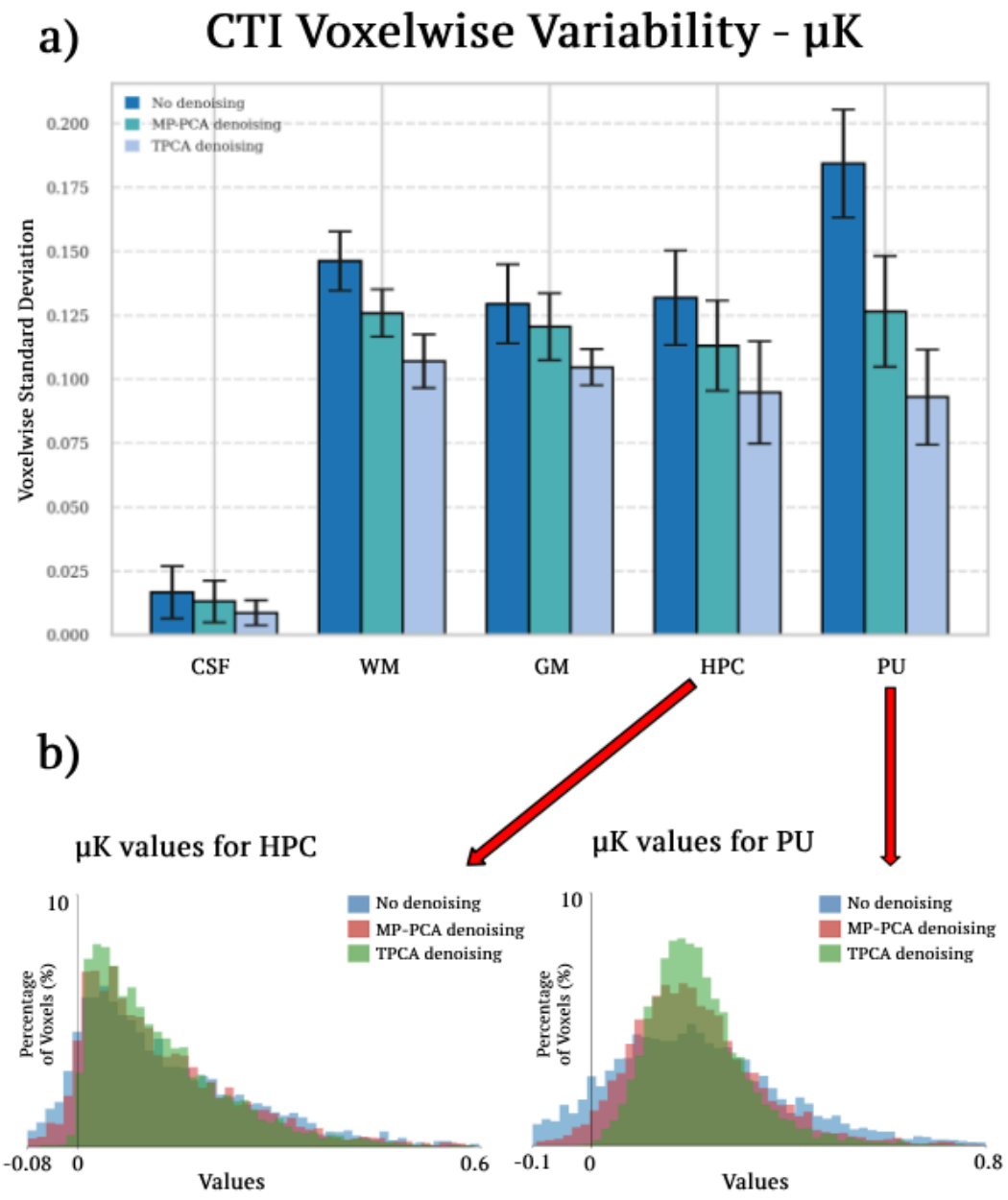


**Figure 2**. Denoising reduces µK variability. (a) µK variability drop (P1 > P2 > P3) across regions. (b) µK distributions in HPC (left) and PU (right). Abbreviations in Table 1.

**Fig 3**

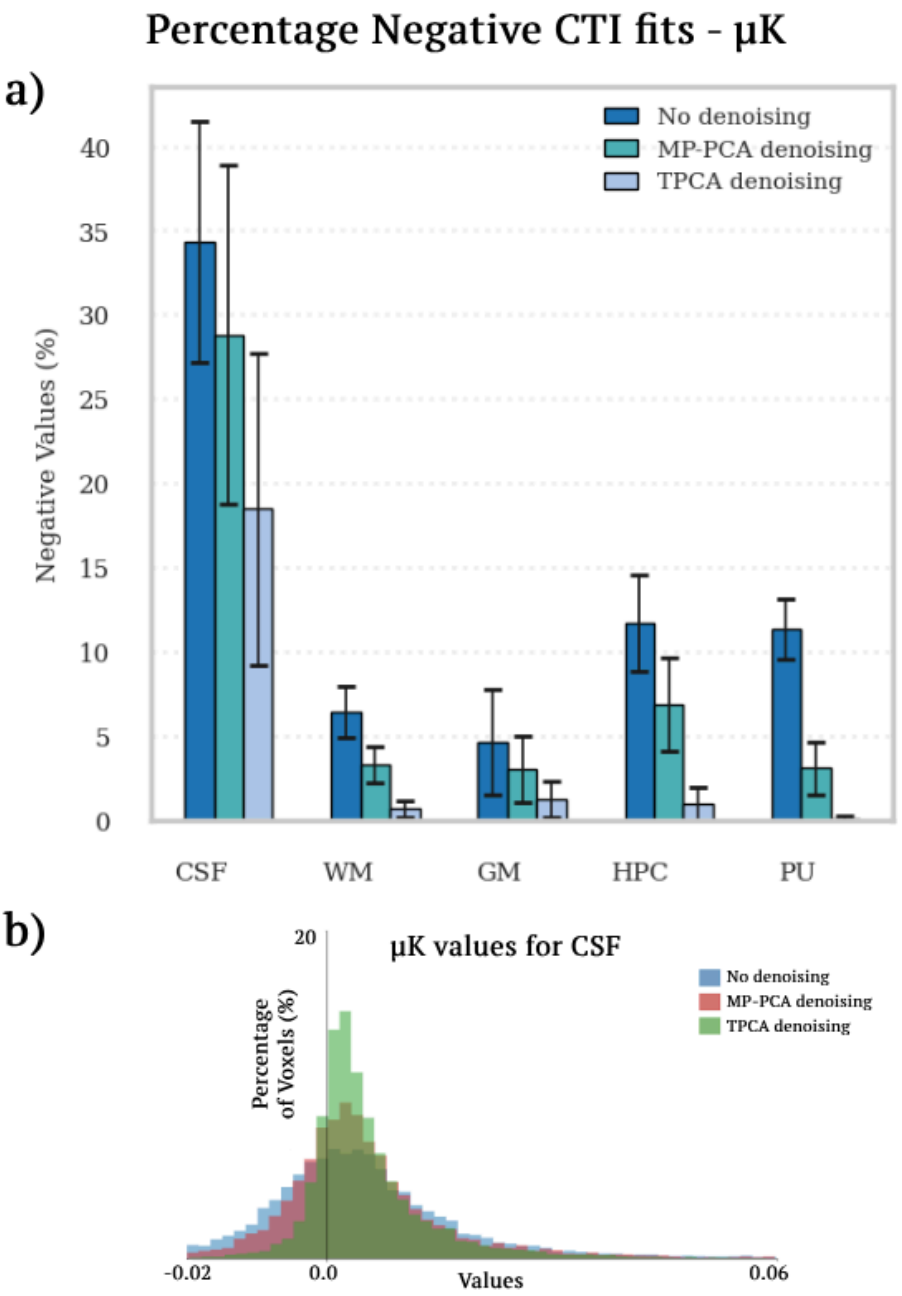


**Figure 3**. Denoising reduces % negative µK fits. (a) P1 > P2 > P3 across regions. (b) CSF µK distribution across pipeline. Abbreviations in Table 1.

## Discussion

Our main findings are twofold. First, PCA-based denoising significantly reduces within-ROI variability of CTI metrics and decreases the number of voxels yielding biologically implausible model fits. Second, these denoising effects are markedly stronger when using TPCA compared to MPPCA. Both effects were consistently observed across gray and white matter regions in healthy young brains. CSF showed

the strongest denoising improvements in terms of reduction of negative fits, maybe related to the fact that Rician denoising was not included. These preliminary results highlight the value of incorporating PCA denoising strategies into the human CTI protocol at 3T to enhance data quality and reliability, in particular TPCA.

**Conclusion**

While these findings are promising, further work is needed to further characterize CTI denoising optimization for clinical and research applications. Future studies will investigate the additional impact of Rician bias correction within the CTI framework on a larger sample, as well as assess how these denoising approaches influence test-retest variability, an important marker of reproducibility.

**Data and Code Availability Statement:**

NIfTI data and analysis code are available upon request to the authors, with the need of a formal sharing agreement.

**References:**


1. Henriques RN, Jespersen SN, Shemesh N (2020) Correlation tensor magnetic resonance imaging. NeuroImage 211:116605.

2. Alves R, Henriques RN, Kerkelä L, Chavarrías C, Jespersen SN, Shemesh N (2022) Correlation Tensor MRI deciphers underlying kurtosis sources in stroke. NeuroImage 247:118833.

3. Novello L, Henriques RN, Ianuş A, Feiweier T, Shemesh N, Jovicich J (2022) In vivo Correlation Tensor MRI reveals microscopic kurtosis in the human brain on a clinical 3T scanner. NeuroImage 254:119137.

4. Veraart J, Novikov DS, Christiaens D, Ades-aron B, Sijbers J, Fieremans E (2016) Denoising of diffusion MRI using random matrix theory. NeuroImage 142:394–406.

5. Henriques RN, Ianuş A, Novello L, Jovicich J, Jespersen SN, Shemesh N (2023) Efficient PCA denoising of spatially correlated redundant MRI data. Imaging Neuroscience 1:1–26.

6. Vos SB, Tax CMW, Luijten PR, Ourselin S, Leemans A, Froeling M (2017) The importance of correcting for signal drift in diffusion MRI. Magnetic Resonance in Med 77:285–299.